

Statistical model for prebreakdown current jumps and breakdown caused by single traps in magnetic tunnel junctions

J. Das, R. Degraeve, G. Groeseneken, S. Stein, H. Kohlstedt, G. Borghs, and J. De Boeck

Citation: *Journal of Applied Physics* **94**, 2749 (2003);

View online: <https://doi.org/10.1063/1.1592300>

View Table of Contents: <http://aip.scitation.org/toc/jap/94/4>

Published by the *American Institute of Physics*



SciLight

Sharp, quick summaries **illuminating**
the latest physics research

Sign up for **FREE!**

AIP
Publishing

Statistical model for prebreakdown current jumps and breakdown caused by single traps in magnetic tunnel junctions

J. Das,^{a),b)} R. Degraeve, and G. Groeseneken^{b)}
Imec, Kapeldreef 75, B-3001 Leuven, Belgium

S. Stein and H. Kohlstedt
Institut für Festkörperforschung, Forschungszentrum Jülich GmbH, 52425 Jülich, Germany

G. Borghs and J. De Boeck
Imec, Kapeldreef 75, B-3001 Leuven, Belgium

(Received 7 October 2002; accepted 23 May 2003)

To obtain reliable magnetic tunnel junctions (MTJs) for sensor and memory applications, the quality of the Al_2O_3 tunnel barrier is extremely important. Here, we studied the reliability of MTJs with a 1.6 nm Al_2O_3 tunnel barrier formed by ultraviolet light assisted oxidation. In the stress measurements, prebreakdown current jumps and, finally, breakdown are observed. We show, by using statistics, that both the current jumps and the final breakdown can be attributed to single trap generation. Moreover, we can relate the current jump height to the trap location. In this way, we reveal the breakdown mechanism in MTJs and illustrate the importance of reliability studies.
 © 2003 American Institute of Physics. [DOI: 10.1063/1.1592300]

The integration of magnetic tunnel junctions (MTJs) into magnetic random access memories (MRAM) will rely on the excellent magnetic and electrical properties of the MTJ. Surprisingly, only few reports on the reliability of MTJs are available. In most present MTJ reliability studies,^{1–4} ramp tests were performed on the MTJs. However, in addition, constant stress tests are better suited to get an insight in the breakdown mechanisms. Furthermore, since different oxidation methods are used to make the (~ 1 nm) Al_2O_3 tunnel barrier in MTJs, we believe that reliability studies are important to investigate Al_2O_3 quality. Recently, preliminary constant voltage tests were performed on naturally oxidized MTJs,⁵ concluding that in this case, breakdown is initiated by extrinsic defects. Here, we will demonstrate that intrinsic breakdown behavior can be obtained by using a different oxidation technique.

We present an in-depth analysis of the degradation and breakdown of MTJs with a 1.6 nm Al_2O_3 tunnel barrier formed by ultraviolet (UV) light-assisted oxidation. We will demonstrate that the reliability concepts used for SiO_2 can also be applied to Al_2O_3 . We will show that the observed degradation is due to the generation of single traps. Finally, we can link the generation of traps, the prebreakdown current through these traps, and the breakdown of MTJs. This study illustrates the fact that breakdown tests can lead to a quality test of the available oxidation methods for MTJs.

Contrary to the Al_2O_3 tunnel barrier in MTJs, the reliability of SiO_2 capacitors is a well-established research topic. It is generally accepted that intrinsic breakdown of thin SiO_2 layers is related to the generation of a percolation path of traps in the oxide.⁶ Recently, evidence has been presented that this mechanism also causes breakdown in thick Al_2O_3

layers.⁷ Applying an electrical stress to the oxide leads to trap generation. At a certain moment, a conduction path of neighboring traps is formed between the two interfaces and, as a result, the oxide breaks down. When scaling down the oxide thickness, fewer traps are needed to form this breakdown path. In the limit, for very thin oxides, only one well-positioned trap is sufficient to trigger a breakdown event. Recently, prebreakdown current steps were observed in stress measurements on small ($2\ \mu\text{m}^2$) SiO_2 capacitors. These are attributed to the creation of two-trap conduction paths, which are physically identical to breakdown paths except that their conductivity is insufficient to cause the electrical runaway effects that accompany breakdown.⁸

The detailed layer sequence of the MTJ stack, used in this study, is the following: Si/SiO_2 substrate/Ta 5 nm/ $\text{Ni}_{80}\text{Fe}_{20}$ 3 nm/ FeMn 20 nm/ $\text{Co}_{90}\text{Fe}_{10}$ 3 nm/ Al 1.3 nm + oxidation/ $\text{Co}_{90}\text{Fe}_{10}$ 3 nm/ $\text{Ni}_{80}\text{Fe}_{20}$ 7 nm/ Cu 5 nm. All layers are deposited by sputtering. To obtain the Al_2O_3 tunnel barrier, the deposited Al layer was exposed to an atmosphere of 5 mbar O_2 and UV light.⁹ MTJs with different top electrode sizes were fabricated. First, the bottom and top electrode are defined by a two-step ion milling. This is followed by a self-aligned SiO_2 passivation step. After a final metalization deposition, which provides contacts to the top and bottom electrodes, an anneal was performed at 250 °C in a magnetic field. The MTJs showed a tunnel-magnetoresistance signal of 30%.

A constant voltage stress at different voltages was applied to the MTJs until breakdown occurred. Figure 1 shows a typical current versus time trace of a stress measurement on a $12.5\ \mu\text{m}^2$ MTJ at 1.1 V. The time-to-breakdown (t_{BD}) is a statistically distributed parameter. The cumulative time-to-breakdown distributions $F(t_{\text{BD}})$ (at stress levels from 1.05 V up to 1.125 V) are fitted with a Weibull function having two parameters: The distribution slope β and the 63% value t_{63} .

^{a)}Electronic mail: jdas@imec.be

^{b)}Also at: Electronic Engineering Department, KULeuven, Belgium.

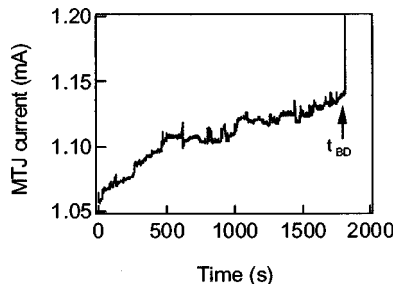


FIG. 1. Typical stress curve ($V=1.1$ V) of a $12.5 \mu\text{m}^2$ MTJ. Several pre-breakdown current jumps are observed before the MTJ finally breaks down at $t=t_{\text{BD}}$.

The measured t_{BD} distributions, together with the Weibull fits, are shown in Fig. 2. As explained in our previous study,⁵ it was necessary to verify the scaling of t_{BD} with the area of the devices. It was found that t_{BD} scales properly with the area, so breakdown due to perimeter effects can be excluded.

From Fig. 1, it is clear that several sudden current jumps are already observed before the final MTJ breakdown occurs. These current jumps are similar to the prebreakdown events in thin SiO_2 ,⁸ and can be further analyzed to provide information on the defect position. It is noteworthy that this defect or trap creates a metastable state in the oxide. Due to the limited oxide thickness, a trapped electron will not remain in this state very long but it will tunnel out rapidly toward the cathode. As a result, traps give rise to additional conduction paths.

For each measurement (at $V=1.1$ V), the time t_i , which corresponds to the first current step larger than ΔI_i , was extracted. In this way, for each ΔI_i , a distribution of t_i was obtained (Fig. 3). All of the distributions were fitted with a maximum likelihood algorithm. The Weibull slope remains constant for all distributions and equals 0.8. We will now develop a model that relates the observed current jumps and breakdown of the MTJ to the generation of traps in Al_2O_3 . Recently, for 2.4 nm SiO_2 capacitors, it was shown that t_i (time to observe a current jump $>\Delta I_i$), is Weibull distributed and the Weibull slope β decreases for decreasing ΔI_i .⁸ These observations were statistically explained with a two-trap percolation model. For ultrathin oxide layers, however,

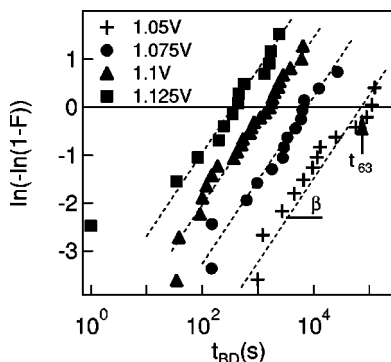


FIG. 2. The distributions of time-to-breakdown (t_{BD}) at different stress levels. The cumulative distributions F are plotted on a Weibull scale: This results in straight lines with slope β . The 63% values of $t_{\text{BD}} (=t_{63})$ are located where the distributions intersect with the zero axis.

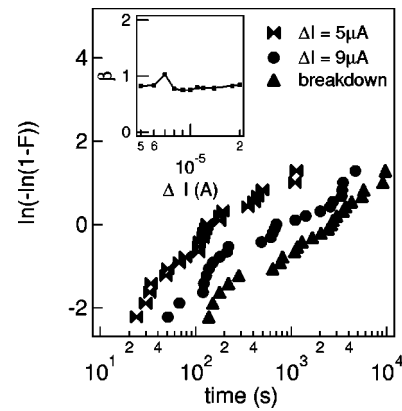


FIG. 3. Distributions of the time t_i to observe the first current step higher than a given current value ΔI_i . As this current gets higher, the Weibull plot shifts to the right-hand side. The right-hand side curve is the breakdown distribution at 1.1 V. The inset shows the Weibull slope β which remains constant.

we expect both the prebreakdown and the breakdown to be triggered by single traps created during the stress. To prove this, we start from a general relation for trap generation similar to that in SiO_2 :⁸

$$D_{\text{ot}} = C t^m, \quad (1)$$

with D_{ot} as the trap density, C as a constant, t as the stress time, and m as the (logarithmic) trap generation rate. For events corresponding to current jumps $>\Delta I_i$, a certain trap density $D_{\text{ot},i}$ is required. For all single trap events ΔI_i , $D_{\text{ot},i}$ is Poisson distributed (= Weibull distributed with slope $\beta = 1$). Poisson distributions for $D_{\text{ot},i}$ can be transformed into Weibull distributions for t_i using Eq. (1). The Weibull slope for these t_i distributions becomes $\beta = m$, a constant for all ΔI_i . This constant slope for the t_i distributions is, hence, a characteristic of the single trap generation and breakdown. This is in contrast with the varying slope observed for multiple trap generation.⁸ Coming back to our experiments, the measured β values are constant for all ΔI_i (Fig. 3). Consequently, we can conclude that all the different prebreakdown current jumps, as well as the final breakdown, are intrinsic degradation effects caused by single trap generation. Note that a β value <1 is usually attributed to extrinsic breakdown mechanisms. However, in this case, we have a generation of single traps, which is an intrinsic degradation mechanism. Using the transformation of Eq. (1), where the trap generation rate $m=0.8$, we clearly see that the creation of single traps leads to a t_i distribution with Weibull slope $\beta = m=0.8$.

We will now derive a relation between the measured current step magnitudes ΔI_i and the position of the traps in the oxide. To achieve this, the percolation concept, as it has been applied for thin SiO_2 , will be extended to model single trap conduction. The current through each conduction path ΔI is determined by the longest trap-to-interface distance x_{perc} as defined in Fig. 4. The probability $P(N, x_{\text{perc}})$ to have a device with exactly N traps (at a density of traps D_{ot}) and at least one single trap percolation path with $x < x_{\text{perc}}$, is given by

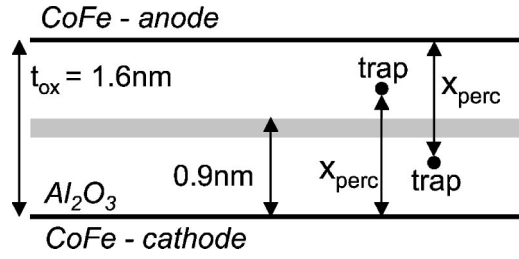


FIG. 4. x_{perc} is defined as the longest distance from the trap to one of both interfaces. If a trap is positioned within the gray part of the tunnel barrier ($x_{\text{perc}} < 0.9$ nm), breakdown will occur.

$$P[N, x_{\text{perc}}] = \left[1 - \left(2 - \frac{2x_{\text{perc}}}{t_{\text{ox}}} \right)^N \right] \cdot \left[\frac{(At_{\text{ox}}D_{\text{ot}})^N}{N!} e^{-At_{\text{ox}}D_{\text{ot}}} \right], \quad (2)$$

with t_{ox} is the oxide thickness and A is the oxide area. Note that the first factor of Eq. (2) gives the probability to have at least one percolation path with $x < x_{\text{perc}}$ in an oxide with exactly N defects and the second factor gives the probability to have exactly N defects. From Eq. (2), we can easily derive the probability to have at least one percolation path with $x < x_{\text{perc}}$, by summing Eq. (2) for $N:1 \rightarrow \infty$ (at fixed D_{ot}). Setting this probability to 0.63, gives the relation between x_{perc} and $D_{\text{ot},63}$:

$$\frac{1}{At_{\text{ox}}D_{\text{ot},63}} = \frac{2x_{\text{perc}}}{t_{\text{ox}}} - 1. \quad (3)$$

This relation gives the average D_{ot} needed to create at least one trap at $x < x_{\text{perc}}$.

Combining Eqs. (1) and (3), x_{perc} can be related to the t_i distribution shown in Fig. 3(a). The constant C in Eq. (1) was calculated (similar as for SiO_2 capacitors)⁸ from the assumption that breakdown occurs when a trap with $x_{\text{perc}} < 0.9$ nm is created. Taking this into account, we can finally construct the current through the traps ($I_{\text{trap}} = \Delta I$) versus x_{perc} (Fig. 5). These results are very useful to reveal the physical conduction mechanism through traps in MTJs, although more inves-

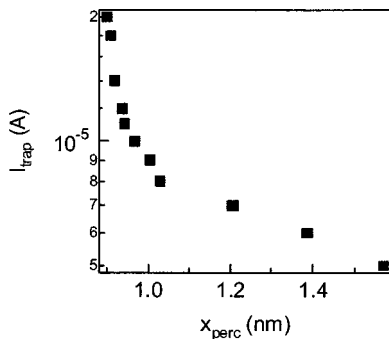


FIG. 5. Relation between the current through the traps (I_{trap}) and the trap position within the barrier (x_{perc}) at stress voltage $V = 1.1$ V.

tigation will be required. We attempted to model this curve by a trap-assisted tunneling model,¹⁰ but unrealistically high trap cross sections were found ($> 10^{-13} \text{ cm}^2$). This proves that at the position of the trap, the tunneling barrier is distorted and the insulating properties are severely affected. We assume that the creation of traps will locally lower the barrier height, which results in a much higher local conductivity. To get additional insight in the trap creation processes, other techniques, like e.g., ballistic electron emission microscopy¹¹ and noise characterization,^{12,13} can be useful, in addition to the electrical stress measurements which give direct quantitative information on MTJ devices.

In summary, we analyzed in detail the reliability of 1.6 nm UV-oxidized Al_2O_3 MTJs. Intrinsic prebreakdown and breakdown were observed after constant voltage stress. These events are caused by the creation of single trap conduction paths and the relation of current versus trap position has been determined applying a percolation concept. Besides the eventual breakdown, the prebreakdown generation of leakage paths will result in a resistance drift of the MTJ and this may jeopardize the MRAM function. This should be taken into account in a reliability prediction. Finally, this study should be extended toward other oxidation techniques (and different oxide thicknesses) to obtain a global quantitative comparison between the available oxidation methods.

One of the authors (J.D.) acknowledges the IWT for financial funding. E. Vandenplas is acknowledged for processing assistance. This work is partly supported by the HGF-Strategiefonds "Magnetoelectronic" and the BMBF-Leitprojekt: "Magnetoelektronik."

- ¹W. Oepts, H. J. Verhagen, W. J. M. de Jonge, and R. Coehoorn, Appl. Phys. Lett. **73**, 2363 (1998).
- ²K. Shimazawa, N. Kasahara, J. J. Sun, A. Araki, H. Morita, and M. Matsuzaki, J. Appl. Phys. **87**, 5194 (2000).
- ³J. Schmalhorst, H. Brückl, M. Justus, A. Thomas, G. Reiss, M. Vieth, G. Gieres, and J. Wecker, J. Appl. Phys. **89**, 586 (2001).
- ⁴B. Oliver, Q. He, X. Tang, and J. Nowak, J. Appl. Phys. **91**, 4348 (2002).
- ⁵J. Das, R. Degraeve, P. Roussel, G. Groeseneken, G. Borghs, and J. De Boeck, J. Appl. Phys. **97**, 7712 (2002).
- ⁶R. Degraeve, J. L. Ogier, R. Bellens, P. J. Roussel, G. Groeseneken, and H. E. Maes, IEEE Trans. Electron Devices **45**, 904 (1998).
- ⁷A. Kerber, E. Cartier, R. Degraeve, L. Pantisano, P. Roussel, and G. Groeseneken, VLSI Technology Symp. Dig. of Techn. Papers, (2002), pp. 76–77.
- ⁸R. Degraeve, B. Kaczer, F. Schuler, M. Lorenzini, D. Wellekens, P. Hendrickx, J. Van Houdt, L. Haspeslagh, G. Tempel, and G. Groeseneken, Tech. Dig. - Int. Electron Devices Meet. **2001**, 6.2.1 (2001).
- ⁹P. Rottländer, H. Kohlstedt, P. Grünberg, and E. Girgis, J. Appl. Phys. **87**, 6067 (2000).
- ¹⁰F. Schuler, R. Degraeve, P. Hendrickx, and D. Wellekens, Int. Reliability Physics Symp. (2002), pp. 26–33.
- ¹¹W. H. Rippard, A. C. Perrella, and R. A. Buhrman, Appl. Phys. Lett. **78**, 1601 (2001).
- ¹²C. T. Rogers and R. A. Buhrman, Phys. Rev. Lett. **55**, 859 (1985).
- ¹³F. Crupi, B. Neri, and S. Lombardo, IEEE Electron Device Lett. **32**, 319 (2000).